

SYNTHESIS AND PROPERTIES
OF INORGANIC COMPOUNDS

Synthesis of Monetite from Calcium Hydroxyapatite
and Monocalcium Phosphate Monohydrate
under Mechanical Activation Conditions

T. V. Safronova^{a, *}, I. S. Sadilov^a, K. V. Chaikun^a,
T. B. Shatalova^a, and Ya. Yu. Filippov^a

^aMoscow State University, Moscow, 119991 Russia

*e-mail: t3470641@yandex.ru

Received January 11, 2019; revised February 17, 2019; accepted March 15, 2019

Abstract—A powder of monetite CaHPO_4 with a particle size of 100–300 nm was synthesized from monocalcium phosphate monohydrate $\text{Ca}(\text{H}_2\text{PO}_4)_2 \cdot \text{H}_2\text{O}$ and calcium hydroxyapatite $\text{Ca}_{10}(\text{PO}_4)_6(\text{OH})_2$ in an acetone medium upon mechanical activation in a planetary mill. According to X-ray powder diffraction data, after heat treatment in the range 900–1100°C, the phase composition of the samples was represented by calcium β -pyrophosphate $\beta\text{-Ca}_2\text{P}_2\text{O}_7$. The synthesized powder can be used for producing resorbable calcium phosphate ceramic materials.

Keywords: powder, phase transformations, calcium pyrophosphate, ceramics

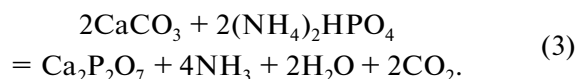
DOI: 10.1134/S0036023619090171

Calcium phosphates are used as nutritional supplements [1] and catalysts for some chemical reactions [2, 3], in agriculture as fertilizers [4], as well as for creating materials with unique properties. Materials with luminescent properties based on calcium pyrophosphate $\text{Ca}_2\text{P}_2\text{O}_7$ are known [5, 6]. Research is underway on the development and application of biocompatible materials based on various calcium phosphates, including calcium hydroxyapatite $\text{Ca}_{10}(\text{PO}_4)_6(\text{OH})_2$, tricalcium phosphate $\text{Ca}_3(\text{PO}_4)_2$, calcium pyrophosphate $\text{Ca}_2\text{P}_2\text{O}_7$, octacalcium phosphate $\text{Ca}_8(\text{HPO}_4)_2(\text{PO}_4)_4 \cdot 5\text{H}_2\text{O}$, brushite $\text{CaHPO}_4 \cdot 2\text{H}_2\text{O}$, monetite CaHPO_4 , and hydrated calcium pyrophosphate $\text{Ca}_2\text{P}_2\text{O}_7 \cdot x\text{H}_2\text{O}$, for the treatment of bone defects [7–9].

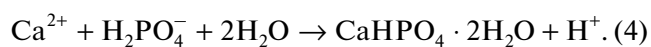
High-quality calcium phosphate powders are synthesized through chemical deposition, thermal conversion, solid-state procedure [10]. In synthesis, additional treatments, such as ultrasonic and hydrothermal treatment [11] and mechanical activation [12], are used. Synthesis of calcium phosphates is carried out in various media, including those mimicking the ionic composition of blood plasma [13]. To produce biocompatible composites, calcium phosphate powders synthesized from mixed-anion solutions are used [14–17].

Regenerative treatment methods require resorbable materials. The solubility of biocompatible calcium phosphates increases with a decrease in the Ca/P molar ratio. For calcium hydroxyapatite $\text{Ca}_{10}(\text{PO}_4)_6(\text{OH})_2$, the molar ratio is Ca/P = 1.67, and

it is a nonresorbable calcium phosphate, known as the inorganic component of bone tissue [18, 19]. For the treatment of bone defects, materials based on tricalcium phosphate $\text{Ca}_3(\text{PO}_4)_2$ with the molar ratio Ca/P = 1.5 are widely used [20]. Researchers also pay attention to calcium phosphates with Ca/P = 1 because of their inherent biocompatibility and higher resorbability. The ratio Ca/P = 1 is inherent to the following calcium phosphates: $\text{Ca}_2\text{P}_2\text{O}_7$, $\text{Ca}_2\text{P}_2\text{O}_7 \cdot x\text{H}_2\text{O}$, CaHPO_4 , and $\text{CaHPO}_4 \cdot 2\text{H}_2\text{O}$. High-temperature calcium pyrophosphate in the form of γ - and β - $\text{Ca}_2\text{P}_2\text{O}_7$ can be produced through thermal conversion of hydrated and/or hydrogen calcium phosphates, as well as through heterogeneous reactions in powder mixtures, including compounds with the Ca/P ratio larger and smaller than 1, for example, by reactions (1) [17], (2) [21], or (3) [22]:



Synthesis of hydrated hydrogen calcium phosphates underlies the production of brushite/monetite cement [23]. The synthesis of brushite or monetite requires the simultaneous presence of Ca^{2+} (from a basic compound) and H_2PO_4^- (from an acidic compound) in the reaction zone:



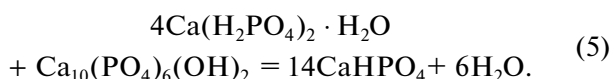
Alkaline calcium sources—tricalcium phosphate $\text{Ca}_3(\text{PO}_4)_2$, calcium hydroxyapatite $\text{Ca}_{10}(\text{PO}_4)_6(\text{OH})_2$, tetracalcium phosphate $\text{Ca}_4(\text{PO}_4)_2\text{O}$, calcium oxide CaO , and calcium hydroxide $\text{Ca}(\text{OH})_2$ —as well as acidic components—phosphoric acid H_3PO_4 , monocalcium phosphate monohydrate $\text{Ca}(\text{H}_2\text{PO}_4)_2 \cdot \text{H}_2\text{O}$, sulfuric acid H_2SO_4 , pyrophosphoric acid $\text{H}_4\text{P}_2\text{O}_7$, and citric acid $\text{C}_3\text{H}_5\text{O}(\text{COOH})_3$ —are presented in review [23]. The choice of components for synthesis calcium phosphate cement, which is intended to be used in situ in non-invasive methods for compensation of bone defects, takes into account the nature of the resulting by-product of the reaction. The use of most of these components taken in any combination leads to the formation of water as a reaction by-product, which is nontoxic for body tissues.

Thus, brushite $\text{CaHPO}_4 \cdot 2\text{H}_2\text{O}$ or monetite CaHPO_4 can be synthesized by reacting solutions of corresponding salts or in pastes in the course of formation of cement stone. The synthesis of hydrogen calcium orthophosphate with the molar ratio $\text{Ca}/\text{P} = 1$ (monetite CaHPO_4) under mechanical activation conditions has not been described to date, although this method affords active powders as a feedstock for production of ceramics or composites with a polymeric matrix.

The present work focuses on the synthesis of calcium phosphate with the molar ratio $\text{Ca}/\text{P} = 1$ (monetite CaHPO_4) from poorly soluble compounds—an acidic calcium salt (monocalcium phosphate monohydrate $\text{Ca}(\text{H}_2\text{PO}_4)_2 \cdot \text{H}_2\text{O}$) and a basic calcium salt (calcium hydroxyapatite $\text{Ca}_{10}(\text{PO}_4)_6(\text{OH})_2$)—under mechanical activation conditions. The use of this pair of precursors enables the production of the powder free of toxic by-products.

EXPERIMENTAL

The amounts of initial salts for the synthesis were determined by reaction (5) leading to calcium phosphate with $\text{Ca}/\text{P} = 1$:



The calculated amounts of hydroxyapatite $\text{Ca}_{10}(\text{PO}_4)_6(\text{OH})_2$ (CAS no. 1306-06-5, puriss. p.a. $\geq 90\%$, Riedel-deHaen, Sigma-Aldrich Laborchemikalien, 04238, lot 70080, Germany) and monocalcium phosphate monohydrate $\text{Ca}(\text{H}_2\text{PO}_4)_2 \cdot \text{H}_2\text{O}$ (CAS no. 10031-30-8 puriss. p.a. $\geq 85\%$, Sigma-Aldrich) were placed in zirconia containers. To a powder mixture, zirconia milling media were added to the weight ratio 1 : 5. Acetone (State Standard GOST 2603-79) was added into the containers with the powders, which were then sealed and fixed in a planetary

mill. The duration of mechanical activation at a revolution rate of 600 rpm was 20 min. After the treatment in the planetary mill, the powder was dried in air at room temperature for 2 h. After drying, the powders were passed through a sieve with a mesh size of 200 μm . From the obtained powders, compact powder pellets 12 mm in diameter and 2–3 mm in height were made at a pressing pressure of 100 MPa without the use of a temporary technological binder using a Carver Laboratory Press model c hand press (United States). The resulting pellets were sintered in a furnace at different temperatures in the range 900–1100°C (heating rate 5 K/min, holding at a given temperature for 2 h, furnace cooling).

Linear shrinkage and geometric density of ceramic samples were determined by measuring their weight and dimensions (with an accuracy of ± 0.05 mm) before and after sintering.

X-ray powder diffraction (XRD) analysis of the initial powders, as-synthesized powder mixtures after mechanical activation, and the samples after sintering was carried out on a Rigaku D/Max-2500 diffractometer with a rotating anode ($\text{CuK}\alpha$ radiation). For qualitative phase analysis, the ICDD PDF2 database [24] was used.

Simultaneous thermal analysis (TA) was carried out on a NETZSCH STA 409 PC Luxx thermal analyzer at a heating rate of 10 K/min. The sample weight was 10 mg. The composition of the gas phase that forms upon the decomposition of the samples was studied using a NETZSCH QMS 403C Aëolos quadrupole mass spectrometer coupled with a NETZSCH STA 409 PC Luxx thermal analyzer. Mass spectra (MS) were recorded for mass numbers 18 and 17 (H_2O^+ and OH^+), 44 (CO_2^+).

The microstructure of the samples was studied by scanning electron microscopy on a Carl Zeiss LEO SUPRA 50VP electron microscope (field emission source); secondary electron images were acquired at an accelerating voltage of 3–20 kV (SE2 detector). A layer of chromium was deposited onto the surface of the samples (up to 10 nm).

RESULTS AND DISCUSSION

Figure 1 shows the X-ray diffraction patterns of the initial reagents and synthesized monetite CaHPO_4 , which indicate that after mechanical activation of the powder mixture in acetone for 20 min, all initial reagent were exhausted to form monetite CaHPO_4 (card PDF 9-80). Indeed, reaction (5) shows that the water amount in the reaction of monocalcium phosphate monohydrate $\text{Ca}(\text{H}_2\text{PO}_4)_2 \cdot \text{H}_2\text{O}$ (card PDF 9-347) and hydroxyapatite $\text{Ca}_{10}(\text{PO}_4)_6(\text{OH})_2$ (card PDF 74-566) is sufficient for the formation of monetite CaHPO_4 . Although both initial compounds have low solubility (~ 17 g/L for $\text{Ca}(\text{H}_2\text{PO}_4)_2 \cdot \text{H}_2\text{O}$ and ~ 0.0003 g/L for

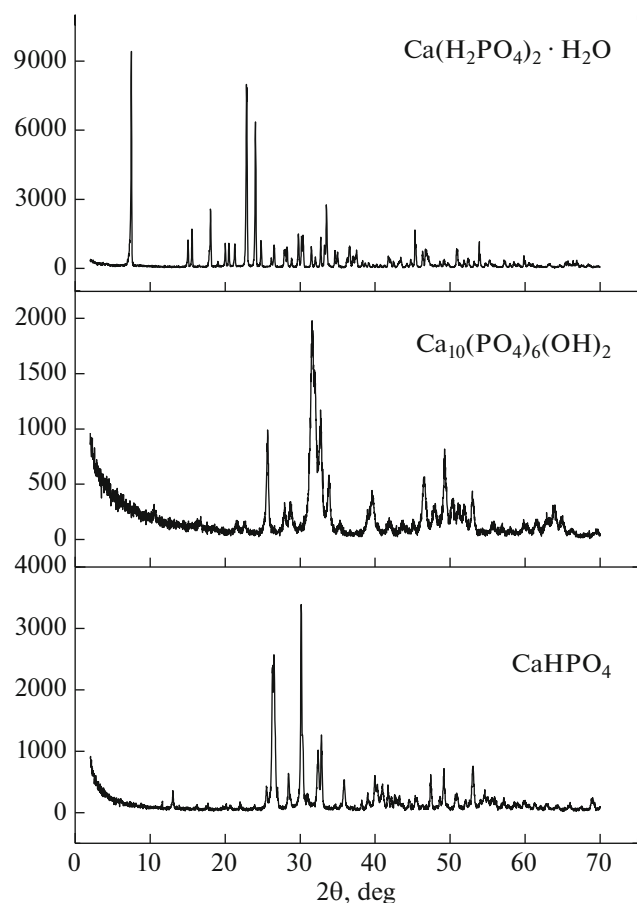
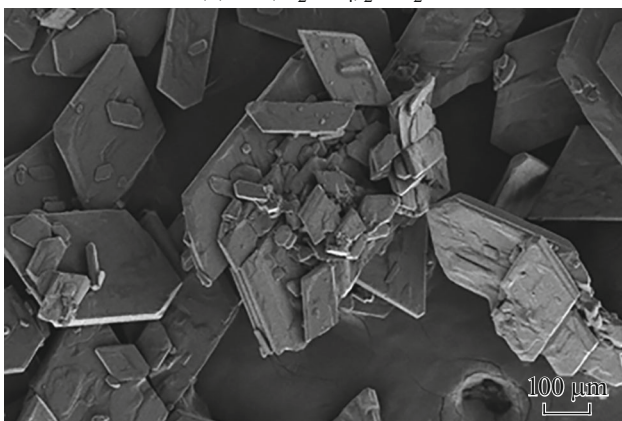


Fig. 1. X-ray powder diffraction patterns of initial compounds— $\text{Ca}(\text{H}_2\text{PO}_4)_2 \cdot \text{H}_2\text{O}$ (card PDF 9-347), and $\text{Ca}_{10}(\text{PO}_4)_6(\text{OH})_2$ (card PDF 74-566)—and the synthesized calcium phosphate CaHPO_4 (card PDF 9-80).

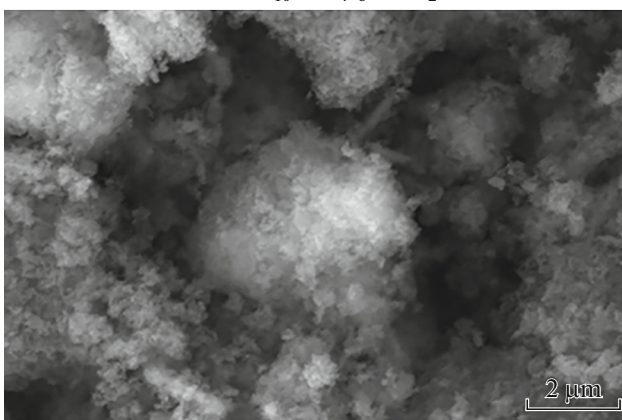
$\text{Ca}_{10}(\text{PO}_4)_6(\text{OH})_2$ [25]), and the amount of water in the reaction zone is small (even with taking into account some amount of water contained in acetone), mechanical activation provides the occurrence of reaction (5). It should be noted that the solubility of monetite CaHPO_4 is intermediate between the solubilities of hydroxyapatite $\text{Ca}_{10}(\text{PO}_4)_6(\text{OH})_2$ and monocalcium phosphate monohydrate $\text{Ca}(\text{H}_2\text{PO}_4)_2 \cdot \text{H}_2\text{O}$, being ~ 0.048 g/L. However, the higher solubility of monocalcium phosphate monohydrate $\text{Ca}(\text{H}_2\text{PO}_4)_2 \cdot \text{H}_2\text{O}$ as compared with the solubility of calcium hydroxyapatite and monetite seems to provide, in aqueous segments (drops) under mechanical activation conditions, the pH level favorable for the formation and persistence of monetite CaHPO_4 rather than hydroxyapatite.

Figure 2 shows SEM images of the initial powders and synthesized monetite CaHPO_4 . The size of monocalcium phosphate monohydrate $\text{Ca}(\text{H}_2\text{PO}_4)_2 \cdot \text{H}_2\text{O}$ plates is rather large, being 50–300 μm at a thickness of 15–20 μm (Fig. 2a). The size of hydroxyapatite

(a) $\text{Ca}(\text{H}_2\text{PO}_4)_2 \cdot \text{H}_2\text{O}$



(b) $\text{Ca}_{10}(\text{PO}_4)_6(\text{OH})_2$



(c) CaHPO_4



Fig. 2. SEM images of initial compounds (a) $\text{Ca}(\text{H}_2\text{PO}_4)_2 \cdot \text{H}_2\text{O}$ and (b) $\text{Ca}_{10}(\text{PO}_4)_6(\text{OH})_2$ and (c) synthesized calcium phosphate CaHPO_4 .

$\text{Ca}_{10}(\text{PO}_4)_6(\text{OH})_2$ particles is 100–200 nm (Fig. 2b). The size of the synthesized monetite CaHPO_4 particles can be estimated at 100–300 nm (Fig. 2c). Two types of particles—of columnar morphology and with the shape close to isometric—are observed in the figure. It is known that monetite CaHPO_4 obtained from solutions is characterized by a lamellar particle mor-

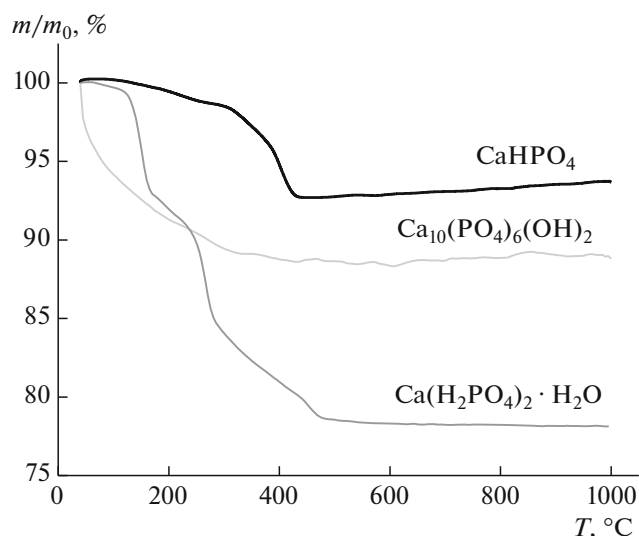


Fig. 3. TA of initial compounds $\text{Ca}(\text{H}_2\text{PO}_4)_2 \cdot \text{H}_2\text{O}$ and $\text{Ca}_{10}(\text{PO}_4)_6(\text{OH})_2$ and synthesized calcium phosphate CaHPO_4 .

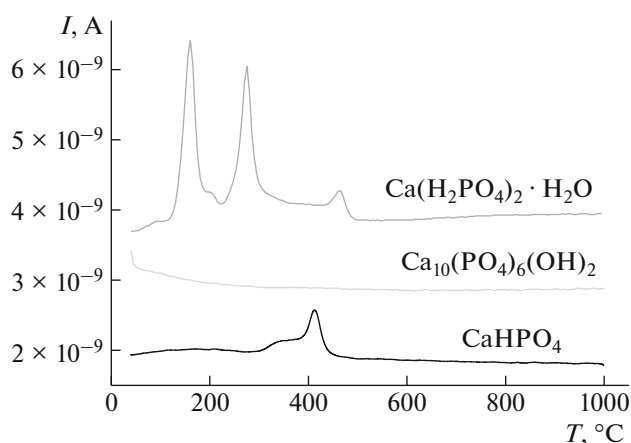


Fig. 4. MS of initial compounds $\text{Ca}(\text{H}_2\text{PO}_4)_2 \cdot \text{H}_2\text{O}$ and $\text{Ca}_{10}(\text{PO}_4)_6(\text{OH})_2$ and synthesized calcium phosphate CaHPO_4 for $m/z = 18$.

phology [26]. In this case, for monetite CaHPO_4 synthesized under mechanical activation conditions from poorly soluble calcium phosphates in the presence of acetone, the lamellar morphology of particles is not observed. This result can be caused by the fact that chemical reaction (5) of synthesis of monetite CaHPO_4 occurs on the surface of hydroxyapatite $\text{Ca}_{10}(\text{PO}_4)_6(\text{OH})_2$. We believe that, under the described conditions, heterogeneous synthesis occurs at the solid/liquid interface, where solid is calcium hydroxyapatite and liquid is an aqueous solution of monocalcium phosphate monohydrate $\text{Ca}(\text{H}_2\text{PO}_4)_2 \cdot \text{H}_2\text{O}$. Acetone functions as a disaggregation medium ensuring the mobility of milling bodies, powder particles, and aqueous solution segments (drops). A certain increase in size of mone-

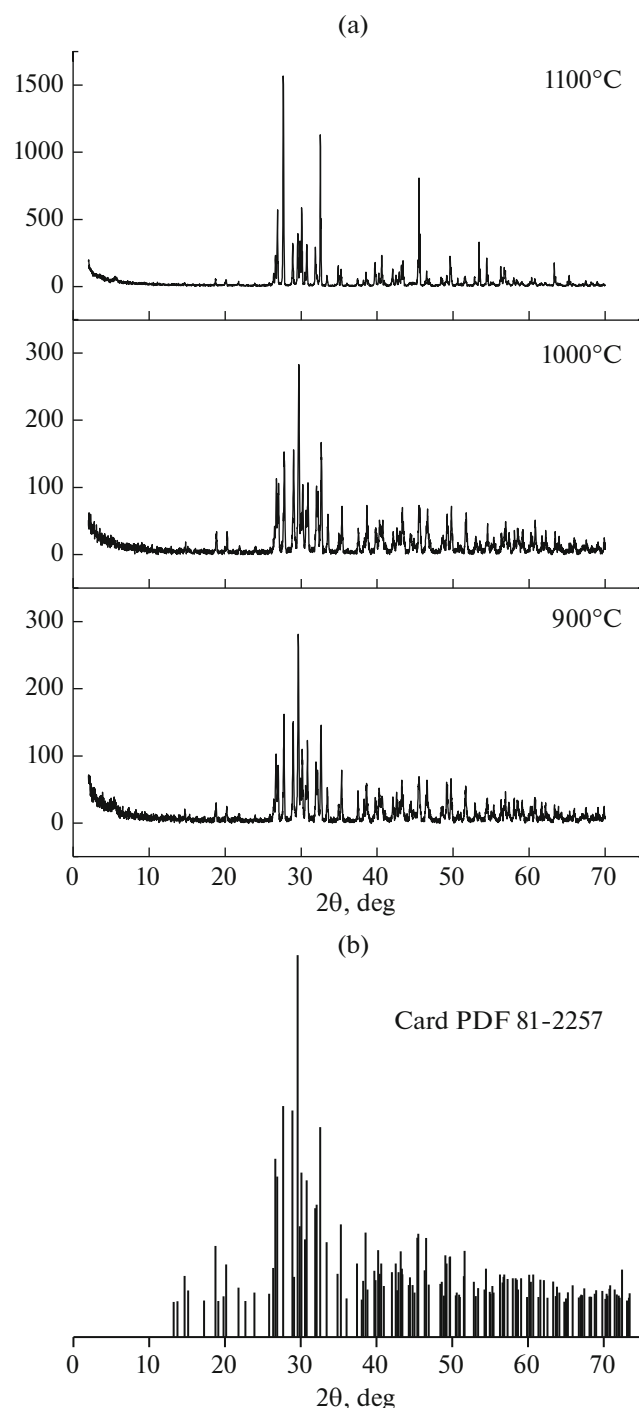
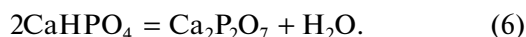


Fig. 5. X-ray powder diffraction patterns of ceramics from the CaHPO_4 powder synthesized from $\text{Ca}(\text{H}_2\text{PO}_4)_2 \cdot \text{H}_2\text{O}$ and $\text{Ca}_{10}(\text{PO}_4)_6(\text{OH})_2$ after heat treatment at (a) 900, 1000, and 1100 °C and (b) and line diagram for card PDF 81-2257 ($\beta\text{-Ca}_2\text{P}_2\text{O}_7$).

tite CaHPO_4 particles as compared with the size of calcium hydroxyapatite $\text{Ca}_{10}(\text{PO}_4)_6(\text{OH})_2$ particles can be caused by the fact that one mole of hydroxyapatite $\text{Ca}_{10}(\text{PO}_4)_6(\text{OH})_2$ ($M = 1004 \text{ g/mol}$) with a density of

3.16 g/cm³ gives rise to 14 moles of monetite ($M = 136$ g/mol) with a density of 2.93 g/cm³. Thus, the volume of a separate particle can increase approximately twofold.

The data of thermal analysis of the initial compounds and synthesized monetite CaHPO₄ are shown in Figs. 3 and 4. The TA and MS data for the initial compounds—Ca(H₂PO₄)₂ · H₂O and Ca₁₀(PO₄)₆(OH)₂—are given for comparison. Comparison of TA and MS data confirm the absence of the initial compounds in the synthesized powder, which is consistent with the XRD data (Fig. 1). For monetite CaHPO₄, reaction (6) of its transformation to pyrophosphate Ca₂P₂O₇ occurs at 400°C.



The total weight loss of monetite CaHPO₄ powder on heating was ~7% (Fig. 3). According to MS data, the weight loss of monetite CaHPO₄ is due to water release in the range 300–475°C (Fig. 4).

According to XRD data (Fig. 5), the phase composition of ceramics after test heat treatments in the temperature range 900–1100°C is represented by β-Ca₂P₂O₇.

Figure 6 presents (a) the linear shrinkage and (b) density of ceramic samples before and after sintering. The density of the sample compacted at 100 MPa from the synthesized powder was 45% of the theoretical density of β calcium pyrophosphate (3.09 g/cm³). The linear shrinkage of the samples after heat treatment at 900°C was 17% and after heat treatment at 1100°C, 25%. The density of the samples after heat treatment at 1000–1100°C was 74–76% as compared with the theoretical density of β calcium pyrophosphate (3.09 g/cm³).

Figure 7 shows the microstructure of ceramics based on β-Ca₂P₂O₇ after heat treatment at different temperatures in the range 900–1100°C. The grain size after heat treatment at 900–1000°C is 2–4 μm. After annealing at 900°C the structure of the ceramics looks more loose and porous. The ceramic grain size after sintering at 1100°C is 5–10 μm.

CONCLUSIONS

The powder of monetite CaHPO₄ with a particle size of 100–300 nm synthesized from monocalcium phosphate monohydrate Ca(H₂PO₄)₂ · H₂O and calcium hydroxyapatite Ca₁₀(PO₄)₆(OH)₂ under mechanical activation conditions can be used for producing ceramic materials with the phase composition containing the biocompatible bioresorbable phase, calcium pyrophosphate β-Ca₂P₂O₇.

In addition, the synthesized powder can be used as a filler to create materials with a polymer matrix, as well as for doping with appropriate ions and as a matrix when creating luminescent materials.

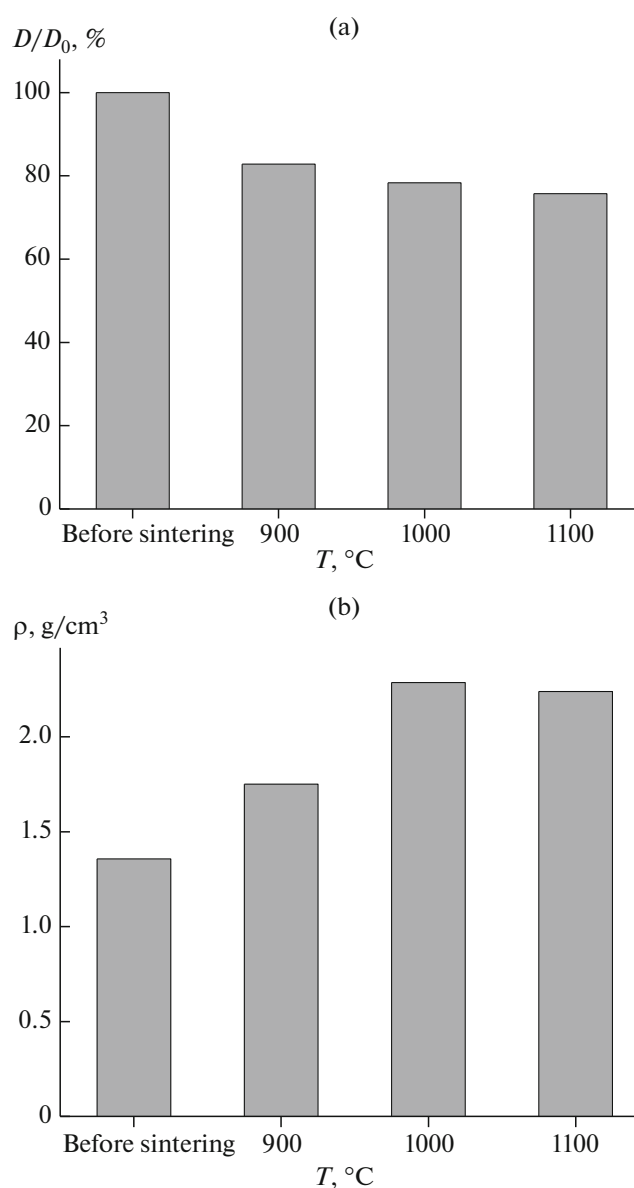


Fig. 6. (a) Linear sizes and (b) density of ceramics from the CaHPO₄ powder synthesized from Ca(H₂PO₄)₂ · H₂O and Ca₁₀(PO₄)₆(OH)₂ after heat treatment at 900, 1000, and 1100°C.

Ceramic calcium phosphate materials obtained from the synthesized powder, containing a bioresorbable and biocompatible phase of calcium pyrophosphate β-Ca₂P₂O₇, can be recommended for creating bone implants.

ACKNOWLEDGMENTS

The work was accomplished using equipment purchased at the expense of the Moscow State University Development Program.

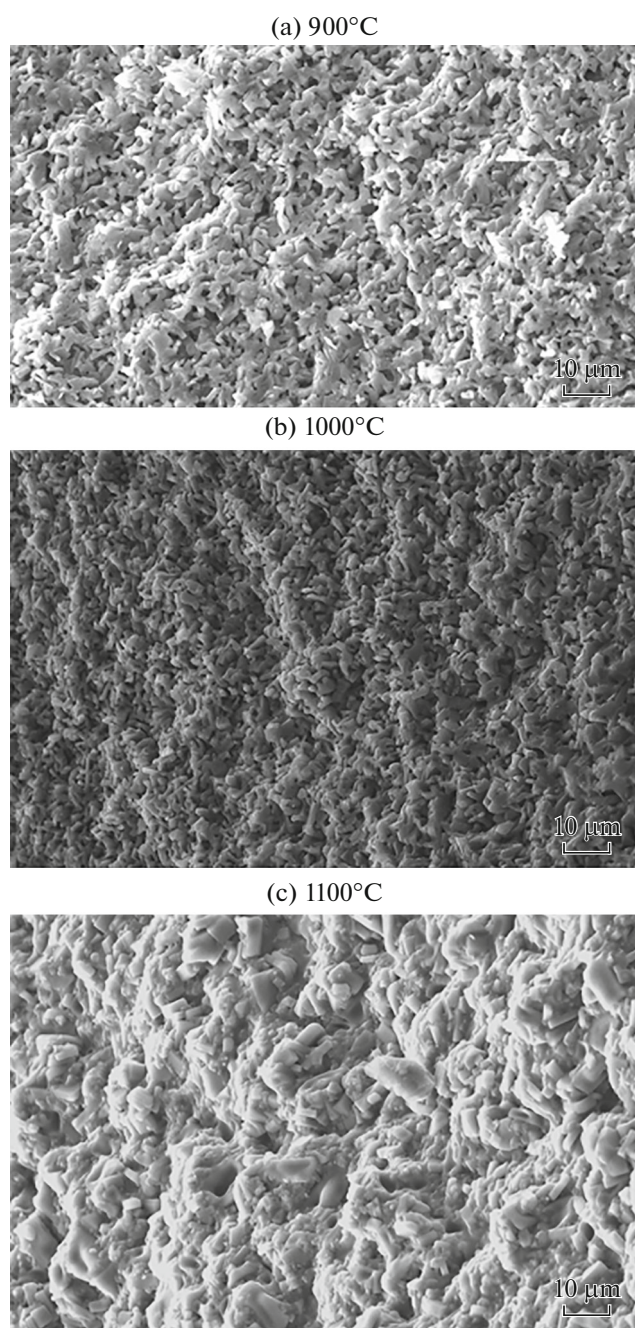


Fig. 7. SEM images of ceramics from the CaHPO_4 powder synthesized from $\text{Ca}(\text{H}_2\text{PO}_4)_2 \cdot \text{H}_2\text{O}$ and $\text{Ca}_{10}(\text{PO}_4)_6(\text{OH})_2$ after heat treatment at (a) 900, (b) 1000, and (c) 1100°C.

FUNDING

The study was supported by the Russian Foundation for Basic Research (project nos. 16-08-01172, 18-29-11079, and 18-53-00034).

CONFLICT OF INTERESTS

The authors declare no conflict of interests.

AUTHOR CONTRIBUTIONS

T.V. Safronova formulated a goal, designed the experiment, and wrote the paper; I.S. Sadilov and K.V. Chaikun synthesized samples and interpreted the XRD data; T.B. Shatalova performed thermal analysis (TA, MS) and interpreted the results; Ya.Yu. Filippov conducted electron microscopic studies of the synthesized powders and samples of ceramic materials. All authors participated in the discussion of the results.

REFERENCES

1. S. I. Kiseleva, *Nutritional and Biologically Active Supplements: A Tutorial* (Izd. NGTU, Novosibirsk, 2013) [in Russian]. ISBN 978-5-7782-2251-9.
2. H. Ruthner and H. Noller, *J. Catal.* **38**, 264 (1975). [https://doi.org/10.1016/0021-9517\(75\)90087-1](https://doi.org/10.1016/0021-9517(75)90087-1)
3. V. C. Ghantani, M. K. Dongare, and S. B. Umbarkar, *RSC Adv.* **4**, 33319 (2014). <https://doi.org/10.1039/c4ra06429a>
4. A. A. Rasulov, O. A. Badalova, U. K. Alimov, et al., *Universum: Tekh. Nauki* **8**, (41), (2017). <http://7universum.com/ru/tech/archive/item/5081>.
5. Basu M. Siddhartha, V. Sudarsana, and A. K. Tyagi, *Solid State Sci.* **85**, 26 (2018). <https://doi.org/10.1016/j.solidstatesciences.2018.09.007>
6. J. Roman-Lopez, I. B. Lozano, E. Cruz-Zaragoza, et al., *Appl. Radiat. Isot.* **124**, 44 (2017). <https://doi.org/10.1016/j.apradiso.2017.03.004>
7. S. V. Dorozhkin, *Ceram. Int.* **41**, 13913 (2015). <https://doi.org/10.1016/j.ceramint.2015.08.004>
8. T. V. Safronova and V. I. Putlyaev, *Inorg. Mater.* **53**, 17 (2017). <https://doi.org/10.1134/S0020168516130057>
9. H. H. Xu, P. Wang, L. Wang, et al., *Bone Res.* **5**, 17056 (2017). <https://doi.org/10.1038/boneres.2017.56>
10. A. Shavandi, A. El. Bekhit, A. Din, et al., *J. Biomim. Biomater. Biomed. Eng.* **25**, 98 (2015). <https://doi.org/10.4028/www.scientific.net/JBBBE.25.98>
11. N. Ouerfelli and M. F. Zid, *J. Struct. Chem.* **57**, 628 (2016). <https://doi.org/10.1134/S0022476616030252>
12. M. V. Chaikina, N. V. Bulina, A. V. Ishchenko, et al., *Russ. Phys. J.* **56**, 1176 (2014). <https://doi.org/10.1007/s11182-014-0159-0>
13. O. A. Golovanova, *Russ. J. Inorg. Chem.* **63**, 1541 (2018). <https://doi.org/10.1134/S0036023618120094>
14. A. P. Solonenko, A. I. Blesman, D. A. Polonyankin, et al., *Russ. J. Inorg. Chem.* **8**, 993 (2018). <https://doi.org/10.1134/S0036023618080211>
15. T. V. Safronova, V. I. Putlyaev, Ya. Yu. Filippov, et al., *Glass Ceram.* **75**, 118 (2018). <https://doi.org/10.1007/s10717-018-0040-7>
16. Z. A. Ezhova, N. A. Zakharov, E. M. Koval, et al., *Russ. J. Inorg. Chem.* **63**, 1001 (2018). <https://doi.org/10.1134/S0044457X18080068>

17. T. V. Safronova, A. V. Knot'ko, T. B. Shatalova, et al., *Glass Ceram.* **73**, 25 (2016).
<https://doi.org/10.1007/s10717-016-9819-6>
18. S. N. Danil'chenko, *Visn. SumDU, Ser. Fiz., Mat., Mekh.*, No. 2, 33 (2007).
19. S. A. Gerk and O. A. Golovanova, *Vestn. Omsk. Univ.*, No. 4 (2015).
20. R. G. Carrodeguas and S. De Aza, *Acta Biomater.* **7**, 3536 (2011).
<https://doi.org/10.1016/j.actbio.2011.06.019>
21. T. V. Safronova, V. I. Putlyaev, S. A. Kurbatova, et al., *Inorg. Mater.* **51**, 1177 (2015).
<https://doi.org/10.1134/S0020168515110096>
22. T. V. Safronova, V. I. Putlyaev, V. K. Ivanov, et al., *Refract. Ind. Ceram.* **56**, 502 (2016).
<https://doi.org/10.1007/s11148-016-9877-x>
23. F. Tamimi, Z. Sheikh, and J. Barralet, *Acta Biomater.* **8**, 474 (2012).
<https://doi.org/10.1016/j.actbio.2011.08.005>
24. ICDD (2010). PDF-4+ 2010 (Database), Ed. by Soorya Kabekkodu, International Centre for Diffraction Data, Newtown Square, PA, USA.
<http://www.icdd.com/products/pdf2.htm>
25. S. V. Dorozhkin, *Prog. Biomater.* **5**, 9 (2016).
<https://doi.org/10.1007/s40204-015-0045-z>
26. R. Mulongo-Masamba, T. El Kassri, M. Khachani, et al., *J. Therm. Anal. Calorim.* **124**, 171 (2015).
<https://doi.org/10.1007/s10973-015-5130-y>

Translated by G. Kirakosyan